RSC Medicinal Chemistry

ROYAL SOCIETY OF CHEMISTRY

RESEARCH ARTICLE

Cite this: *RSC Med. Chem.*, 2023, **14**, 1131

Antileishmanial evaluation of triazole–butenolide conjugates: design, synthesis, *in vitro* screening, SAR and *in silico* ADME predictions†

Alka Raj Pandey,[ae] Suriya Pratap Singh,[a] Karthik Ramalingam,[b] Kanchan Yadav,[c] Amol Chhatrapati Bisen,[df] Rabi Sankar Bhatta,[df] Mrigank Srivastava,[c] Renu Tripathi,[c] Neena Goyal[b] and Koneni V. Sashidhara *[aef]

Received 23rd December 2022,
Accepted 25th March 2023

DOI: 10.1039/d2md00464j

rsc.li/medchem

In the quest to discover novel scaffolds with leishmanicidal effects, a series of 23 compounds containing the most promising 1,2,3-triazole and highly potent butenolide in one framework were synthesized. The synthesized conjugates were screened against *Leishmania donovani* parasite; five of them showed moderate antileishmanial activity against promastigotes (IC_{50} 30.6 to 35.5 μM) and eight of them exhibited significant activity against amastigotes (IC_{50} ≤12 μM). Compound **10u** was found to be the most active (IC_{50} 8.4 ± 0.12 μM) with the highest safety index (20.47). The series was further evaluated against *Plasmodium falciparum* (3D7 strain) and seven compounds were found to be moderately active. Among them, again **10u** emerged as the most active compound (IC_{50} 3.65 μM). In antifilarial assays against adult female *Brugia malayi*, five compounds showed grade II inhibition (50–74%). Structure–activity relationship (SAR) analysis suggested a substituted phenyl ring, triazole and butenolide as essential structural features for bioactivity. Moreover, the results of *in silico* ADME parameter and pharmacokinetic studies indicated that the synthesized triazole–butenolide conjugates abide by the required criteria for the development of orally active drugs, and thus this scaffold can be used as a pharmacologically active framework that should be considered for the development of potential antileishmanial hits.

Introduction

Leishmaniasis, an endemic and one of the world's 20 neglected tropical diseases (NTDs), as declared by the WHO, generally arises by infection with an obligate intramacrophage protozoan parasite of the genus *Leishmania* and transmitted among human beings by a female phlebotomine class of sandflies.[1] On the basis of the type of parasite species involved, degree of morbidity, cell-mediated immunity and tolerance and mortality rate, this protozoan-borne disease exists in three clinical forms, *i.e.*, visceral (VL), cutaneous (CL) and mucocutaneous. *Leishmania major* (Lm) causes cutaneous leishmaniasis which is generally non-fatal but may lead to everlasting blemishes and disfigurement, whereas mucocutaneous leishmaniasis is progressive in nature and ends up with causing both skin and mucosal ulceration. On the other hand, the third clinical form of leishmaniasis, *i.e.* visceral leishmaniasis (VL), is caused by *Leishmania donovani* (Ld). It is commonly known as kala-azar, black fever, and dumdum fever and is considered as the most lethal form if left untreated. In the absence of treatment, the immune system of the host fails which allows VL to become fatal. The leishmania parasite completes its life cycle in humans (host) and sandflies (vector).[2] During the process of feeding on an infected host, the parasite enters into the digestive tract of sandflies, where it multiplies and transforms into extracellular flagellated promastigotes. These infected flies, when feeding on healthy human beings for blood, transfer the promastigotes to the respective mammalian host. Once the parasite enters the host, they start multiplying inside the phagolysosomal compartment of macrophages and transform into a non-motile form, known as amastigote. This form of

[a] *Medicinal and Process Chemistry Division, CSIR-Central Drug Research Institute, BS-10/1, Sector 10, Jankipuram Extension, Sitapur Road, Lucknow 226031, U.P, India. E-mail: kv_sashidhara@cdri.res.in; Fax: +91 522 2771942/2771970; Tel: +91 522 2772450, ext. 4684*

[b] *Division of Biochemistry and Structural Biology, CSIR-Central Drug Research Institute, BS-10/1, Sector 10, Jankipuram Extension, Sitapur Road, Lucknow 226031, U.P, India*

[c] *Division of Molecular Microbiology and Immunology, CSIR-Central Drug Research Institute, Lucknow 226031, U.P, India*

[d] *Pharmaceutics and Pharmacokinetics Division, CSIR-Central Drug Research Institute, Lucknow 226031, U.P, India*

[e] *Sophisticated Analytical Instrument Facility & Research, CSIR-Central Drug Research Institute, BS-10/1, Sector 10, Jankipuram Extension, Sitapur Road, Lucknow 226031, U.P, India*

[f] *Academy of Scientific and Innovative Research (AcSIR), Ghaziabad-201002, U.P, India*

† Electronic supplementary information (ESI) available. See DOI: **https://doi.org/10.1039/d2md00464j**

the parasite has a latent capability for survival under extreme stressful conditions, lysing macrophages and then entering new cells of the host *via* phagocytosis.[3] According to the latest report by the WHO, around 12 million people are affected by all the three different clinical forms of leishmaniasis on the whole in 98 countries, and approximately 1 billion of the population is at high risk of infection.[4] Moreover, on the basis of the number of deaths, after malaria, visceral leishmaniasis is the second life-threatening parasitic disease with a mortality rate of 30 000 deaths per year worldwide.[5] Apart from this, the social disgrace associated with disabilities and deformities such as disfiguring scars, arising due to leishmaniasis, promulgate a societal burden and may hamper overall socioeconomic productivity and development.

Since, despite substantial efforts made by government, non-government and non-profit institutions in the discovery of more effective therapeutic agents, no single vaccine has been proved to be efficacious either for the prevention of leishmaniasis in the host or for vector control, chemotherapy remains the sole weapon, which is effective against leishmaniasis. Moreover, a limited armory of drugs is in use for the treatment, *i.e.*, pentavalent antimonials, amphotericin B, pentamidine, paromomycin and miltefosine. Among these, pentavalent antimonials (Pentostam and Glucantime) used to be the first-line drugs for VL for more than fifty years, but increased rates of resistance and its contraindication of use in patients above 50 years, people with existing problems such as cardiopathy, liver disease and nephropathy and pregnant women led to its declined use. Hence, different liposomal formulations of amphotericin B, an aminoglycoside class of antibiotic, *i.e.*, pentamidine, paromomycin and miltefosine, are used as alternative therapeutic regimens. Although miltefosine, which was initially developed as an anticancer agent, is the only drug which is orally active and highly efficacious with up to 98% cure rates, unfortunately, like antimonials it is associated with therapeutic failure and emergence of resistance. Additionally, the above-described drugs are associated with several disadvantages such as low efficacy, gastrointestinal side effects, toxicity, high cost, teratogenicity, long elimination half-life, longer duration of administration and emergence of resistance with longer use. Hence, the limited portfolio of existing antileishmanial drugs, which are associated with several serious issues, calls for an urgent need for the development of an antileishmanial drug which is novel, safer, more efficacious, cheaper, and devoid of the aforementioned adverse effects as well as effective in killing the intracellular form of leishmanial protozoa.[6]

One of the most versatile and nitrogen-based heterocyclic classes that has been well exploited for the generation of medicinally important scaffolds is 1,2,3-triazole. Its derivatives are well known for exhibiting various biological activities such as anti-HIV, antimicrobial, anticancer, antileishmanial *etc.* In view of antileishmanial reports, several examples can be quoted. For example, Tahghighi *et al.* reported 5-(5-nitrofuran-2-yl)-1,3,4-thiadiazol-2-amines containing *N*-[(1-benzyl-1*H*-1,2,3-triazol-4-yl)methyl] compound (**1**) which is active against *L. major*; Ferreira *et al.* reported difluoromethylene 1,2,3-azole derivative (**2**), active against *L. donovani*; Cassamale *et al.* reported a 1,4-diaryl-1,2,3-triazole analogue (**3**), active against *L. amazonensis* and *L. infantum*; and many more.[7] On the other hand, the butenolide scaffold, abundantly found to be a part of natural and natural product-based structures, bears biodynamic properties and is well known for exhibiting various pharmacological activities such as anticancer, antileishmanial, antimicrobial, antidyslipidemic, antimalarial, *etc.* In particular, the antileishmanial reports on natural products containing a butenolide scaffold, such as terrenolide S (**4**) from endophytic fungus *Aspergillus terreus* against *L. donovani*, andrographolide (**5**) against *L. martiniquensis* and *L. donovani*, and 16α-hydroxycleroda-3,13 (14) *Z*-dien-15,16-olide (**6**) from *Polyalthia longifolia* against *L. donovani*, clearly indicated their therapeutic potential.[8,9] Hence, the antileishmanial reports of 1,2,3-triazole containing heterocycles as well as butenolide-based compounds prompted us to exploit the molecular hybridization approach to design, synthesize and assess 1,2,3-triazole–butenolide conjugates for antileishmanial activity, as such conjugates have not been explored to date for their leishmanicidal effect (Fig. 1).

Results and discussion

Chemistry

A general route for the synthesis of 1,2,3-triazole–butenolide conjugates is presented in Scheme 1. For the introduction of the butenolide ring, mucochloric acid was chosen for the following reasons: numerous reports of the medicinal activity of its derivatives and commercial availability.[10,11] Their synthesis commenced with protection of the hydroxy group of mucochloric acid with the *tert*-butyldimethylsilyl group using *tert*-butyldimethylsilyl trifluoromethanesulfonate (TBDMSOTf) in the presence of 2,6-lutidine as a base in dichloromethane to afford *O*-protected mucochloric acid **7a**.[12] This TBDMS-protected mucochloric acid was then allowed to react with propargyl amine in dimethylformamide (DMF) solvent for the introduction of an alkyne functionality *via* a simple nucleophilic substitution reaction to obtain **8a**.[13] Then, the obtained alkyne-substituted mucochloric acid was allowed to react with different aromatic azides according to a click reaction protocol in the presence of sodium ascorbate and copper sulphate pentahydrate in DMF to afford 1,2,3-triazole containing *O*-protected butenolide derivatives **9a**–**9w**, which were then allowed to undergo deprotection using tetra-*n*-butylammonium fluoride (TBAF) in tetrahydrofuran (THF) at −30 °C to afford the desired 1,2,3-triazole–butenolide derivatives **10a**–**10w** as enantiomeric mixtures.[3,12] For the development of a structure–activity relationship (SAR) and better understanding of the importance of the role of triazole in the activity, one derivative without the 1,2,3-triazole moiety was synthesized by deprotection of *O*-protected alkyne-substituted mucochloric acid **11a**. The structures of all the newly synthesized 1,2,3-triazole–butenolide derivatives were characterized by NMR spectroscopy (^{1}H NMR, ^{13}C NMR and 2D NMR) and high-resolution mass spectrometry (HRMS) and were found to be more than 95% pure as shown by HPLC.

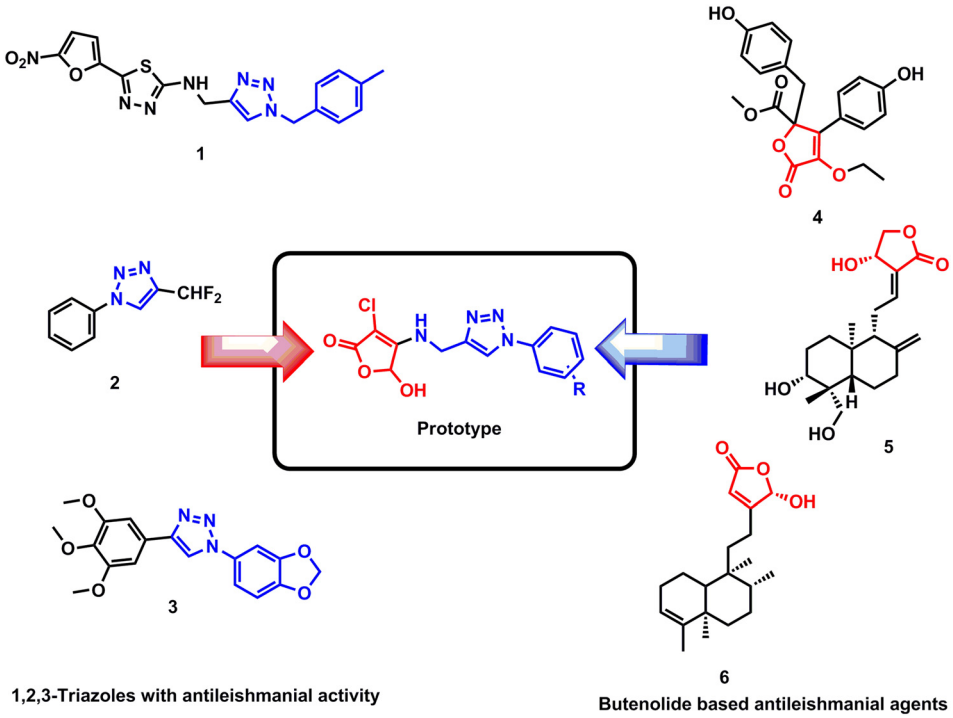

Fig. 1 Rationale for designing 1,2,3-triazole–butenolide conjugates.

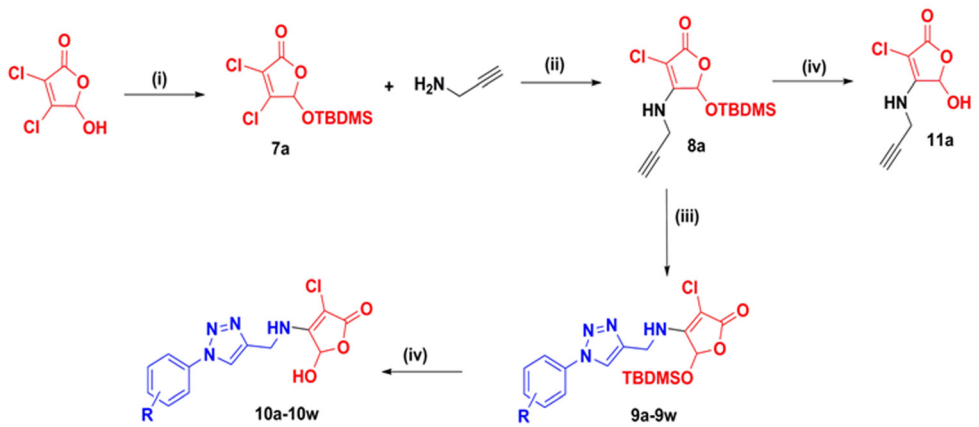

Compd	R	Compd	R	Compd	R	Compd	R
10a	4-OCH_3	**10g**	4-*tert* butyl	**10m**	3,4-Cl	**10s**	3,4,5-OCH_3
10b	H	**10h**	2,4,6-CH_3	**10n**	3-Cl, 4-F	**10t**	3,4-CH_3
10c	4-CH_3	**10i**	3,4-OCH_3	**10o**	3-CF_3	**10u**	3,4-F
10d	4-C_2H_5	**10j**	4-*iso* propyl	**10p**	methylenedioxy	**10v**	2-phenoxy
10e	4-Cl	**10k**	2,5-CH_3	**10q**	4-n-butyl	**10w**	3-F, 4-CH_3
10f	4-F	**10l**	3-CF_3, 4-F	**10r**	2-NO_2		

Scheme 1 Synthesis of 1,2,3-triazole–butenolide conjugates. Reagents and conditions: (i) TBDMSOTf, 2,6-lutidine, DCM, r.t., 1 h; (ii) DMF, r.t., 2 h; (iii) aromatic azides, sodium ascorbate, copper sulphate pentahydrate, DMF, 60 °C, 1 h; (iv) TBAF, THF, −30 °C, 1 h.

Biological studies

***In vitro* antileishmanial activity.** Antileishmanial screening under *in vitro* conditions is generally being done against two stages of the parasite, extracellular promastigotes (as the primary screen) and intracellular amastigotes (as the secondary screen). The amastigote stage is able to survive the hostile environment

Table 1 *In vitro* antileishmanial activity of **10a–10w** and **11a**

Compound code	IC_{50}[a] (μM)		CC_{50}[b] (μM)	SI[c]
	Antipromastigote	Antiamastigote		
10a	≥50	≥25	ND[e]	ND
10b	≥50	NI[d]	ND	ND
10c	≥50	NI	ND	ND
10d	≥50	NI	ND	ND
10e	≥50	≥50	ND	ND
10f	≥50	NI	ND	ND
10g	≥50	≥25	ND	ND
10h	≥50	≥20	ND	ND
10i	NI	NI	ND	ND
10j	NI	≥50	ND	ND
10k	≥50	≥50	ND	ND
10l	30.6 ± 0.14	9.02 ± 0.19	135.5 ± 0.70	15.02
10m	34.1 ± 0.42	8.63 ± 0.08	84.15 ± 0.07	9.75
10n	35.5 ± 1.83	10.55 ± 0.21	77.95 ± 1.62	7.38
10o	32.4 ± 0.42	8.45 ± 0.15	102 ± 1.41	12.07
10p	≥50	≥50	ND	ND
10q	≥50	NI	ND	ND
10r	≥50	≥25	ND	ND
10s	≥100	11.3 ± 0.14	84.75 ± 0.77	7.5
10t	32.5 ± 0.21	10.09 ± 0.28	93.55 ± 0.77	9.27
10u	≥50	8.4 ± 0.12	172 ± 1.41	20.47
10v	≥50	≥20	ND	ND
10w	≥50	≥20	ND	ND
11a	≥50	11.35 ± 0.35	97.25 ± 0.35	8.56
Miltefosine[f]	8.05 ± 1.01	9.42 ± 0.41	52.1 ± 1.53	5.53

[a] IC_{50} (μM): concentration corresponding to 50% growth inhibition of the parasite. [b] Concentration corresponding to 50% cytotoxicity against the J774A cell line. Both IC_{50} and CC_{50} values are the average of three independent assays expressed as average ± standard deviation. [c] Selectivity index (SI): IC_{50} values of cytotoxic activity/IC_{50} values of the anti-amastigote antileishmanial activity. [d] NI: no inhibition. [e] ND: not determined. [f] Miltefosine was used as the standard.

of macrophages and hence needs to be targeted within the host. Thus, to evaluate the antileishmanial activity of 23 compounds of the triazole–butenolide conjugate series, they were tested *in vitro* against both extracellular promastigote and intracellular amastigote stages of luciferase-expressing *L. donovani*.[14] Table 1 depicts the preliminary *in vitro* antileishmanial screening data. Among all the compounds, only five compounds showed moderate antileishmanial activity against promastigotes with an IC_{50} value ranging from 30.6 to 35.5 μM. On the other hand, eight compounds exhibited significant antileishmanial activity against amastigotes with an IC_{50} value of ≤12 μM. The compounds exhibited significantly higher activity against intracellular amastigotes than promastigotes. Interestingly, compound **10u** showed very little activity (IC_{50} >50 μM) against promastigotes as compared to the other compounds. Sometimes promastigote screening fails to identify the compounds that depend on their activity in macrophage metabolic processing.[15] Examples are the pentavalent antimonial sodium stibogluconate,[14,16,17] a prodrug that is converted to toxic SbIII within macrophages, and tannins and related compounds that exert their antileishmanial activity due to macrophage activation.[18] Accordingly, compound **10u** may also depend on host–parasite interaction for its antileishmanial activity. Moreover, only three compounds (**10l**, **10o**, **10u**) were found nontoxic to J774A.1 cells as their safety index was more than 10. The safety index of a compound is defined as the ratio of the cytotoxicity/inhibitory activity in intracellular amastigotes.[19]

***In vitro* antimalarial and antifilarial activity.** Results of *in vitro* evaluation of 1,2,3-triazole–butenolide conjugates against the leishmanial parasite *L. donovani* prompted us to explore their biodynamics and evaluate their antiparasitic potential against other parasites such as *P. falciparum* and female *B. malayi* which are responsible for causing the deadly parasitic diseases malaria and filariasis, respectively. From *in vitro* evaluation against the 3D7 sensitive strain of *P. falciparum*, it was found that seven compounds showed moderate antimalarial activity (Table 2) with IC_{50} values of less than 5 μM: **10a** (IC_{50} = 4.90 μM), **10f** (IC_{50} = 4.42 μM), **10g** (IC_{50} = 4.40 μM), **10k** (IC_{50} = 4.57 μM), **10p** (IC_{50} = 4.34 μM), **10u** (IC_{50} = 3.65 μM), and **10v** (IC_{50} = 4.65 μM).[20] On the other hand, only five compounds showed grade II inhibition (50–74%) in MTT reduction assay when tested against adult female *B. malayi*, *i.e.*, **10m** (52%), **10p** (52%), **10t** (52%), **10w** (66%), and **11a** (65%).[21]

Table 2 *In vitro* antimalarial and antifilarial activity of 1,2,3-triazole–butenolide conjugates

Compd	*P. falciparum* IC_{50} (μM)	Compd	*P. falciparum* IC_{50} (μM)	Compd	*B. malayi* % inhibition in MTT reduction
10a	4.90	**10u**	3.65	**10m**	52
10f	4.42	**10v**	4.65	**10p**	52
10g	4.40			**10t**	52
10k	4.57			**10w**	66
10p	4.34			**11a**	65

Structure–activity relationship (SAR) analysis. On the basis of *in vitro* analysis of the 23 synthesized compounds against both forms of *L. donovani*, a structure–activity relationship (SAR) analysis was performed and concluded. Among the tested compounds, only seven rationalized compounds were active and the rest showed insignificant activity. These active compounds had either a di- or a monosubstituted phenyl ring attached to the triazole side chain. Halogenated and dimethyl substituents particularly at either 3- or at both 3, 4-positions (**10l**, **10m**, **10n**, **10o**, **10u**) favoured the activity. Unsubstituted phenyl rings (**10b**) did not show any inhibition of the amastigote form of the parasite; in contrast, compounds with mono-substitution at the 4-position (**10a**, **10c**, **10d**, **10e**, **10f**, **10g**, **10j**) or the 2-position (**10r** and **10w**) or di-substitution at the 2,5-position (**10k**) were all found inactive. Compounds with 3,4,5-trisubstitution (**10s**) showed inhibition, while 2,4,6-trisubstituted compounds (**10h**) failed in the assay. Also, precursor compound **11a** was found active but was comparatively less active than the final hybrid compounds. Thus, the results of *in vitro* antileishmanial screening clearly suggested that the triazole and butenolide rings are both essential to show inhibition, and disubstituted phenyl rings with a halogen or methyl substituent favours activity.

Considering the *in vitro* screening results of the antimalarial assay, it was found that the substitution in the phenyl side chain was essential for activity as the unsubstituted ring (**10b**) was devoid of activity. Further, the *n*-alkyl substituent in the phenyl ring (**10c**, **10d**, and **10q**) did not produce any effect but the *t*-butyl group (**10g**) had a significant effect on activity. Similarly, the chlorinated phenyl ring (**10e**, **10n**) did not show activity but the fluorinated ring (**10u**) showed maximum potency. Hence, it could be deduced that mono- and disubstituted phenyl rings in the side chain of the triazoyl moiety are essential for activity. In particular, the 3,4-difluorinated phenyl derivative was found to be the most favorable substituent amongst all to show maximum efficacy.

From the *in vitro* antifilarial activity screening results, it was deduced that the 3,4-disubstituted phenyl side ring with alkyl or halogen favoured the activity as compounds **10m**, **10p**, **10t** and **10w** showed moderate inhibitory effects. The combined SAR for all the parasitic diseases is depicted in Fig. 2.

***In silico* ADME study.** In the process of drug discovery, it has been indicated that approximately 40% of the hits abort in clinical trials because of poor pharmacokinetic profile. Hence, absorption, distribution, metabolism and excretion (ADME) data have a compelling importance in the drug discovery process. Apart from this, the cost of discovery projects of new drugs is also affected due to these late-stage failures of drugs in clinical trials. Therefore, it is necessary to detect problematic molecules in the initial stage of the drug discovery process to reduce the risk of late-stage failures and to make the ongoing drug discovery process cost-effective without affecting the budgets of new drug discovery campaigns by enhancing the desired ADME properties through early prediction. Hence, for filtering out and optimising the leads with the desired ADME profile, the *in silico* approach proves to be cost-effective in the drug discovery process. With this aim, an *in silico* study of 1,2,3-triazole–butenolide conjugates (**10a–10w** and **11a**) was carried out for determination of their ADME profiles and the values thus obtained are summarised in Table 3. Analysis of pharmacokinetically relevant properties like topological polar surface area (TPSA), molecular volume (MV) and Lipinski's rule of five using the Molinspiration web tool[22] was carried out. Also, absorption (% ABS) was calculated by using the formula % ABS = 109 − (0.345 × TPSA). After calculation of all the parameters as mentioned above, it could be interpreted that all the synthesized compounds exhibited a good % absorption profile, *i.e.*, 62.39–88.79%. The most active antileishmanial compounds **10m**, **10o** and **10u** showed 78.19% absorption. According to Lipinski's rule of five, any molecule to be developed as an orally active drug candidate should not show more than one violation of the following four criteria: logP (octanol–water partition coefficient) ≤5, molecular weight ≤500, number of hydrogen bond acceptors ≤10 and number of hydrogen bond donors ≤5. From the calculated *in silico* ADME parameters, it was clear that none of the synthesized compounds violated Lipinski's rule of five and thus represented the possibility of the synthesized series for development of a compound with drug-like properties. The TPSA is a parameter for the prediction of how drugs are transported; specifically, it represents the passive mode of transportation of drugs. Moreover, if TPSA ≤ 140 Å^2, the compounds are expected to have good oral bioavailability. 1,2,3-Triazole–butenolide conjugates showed TPSA values ranging between 58.56 and 135.10 Å^2, which represented good permeability of compounds across the cells. Hence, from the results of *in silico* ADME parameters (Table 3) it can be inferred that the synthesized triazole–butenolide conjugates abide by the required criteria for the development of orally active drugs, and thus this scaffold can be used as a pharmacologically active framework that should be considered for the development of potential antileishmanial hits.

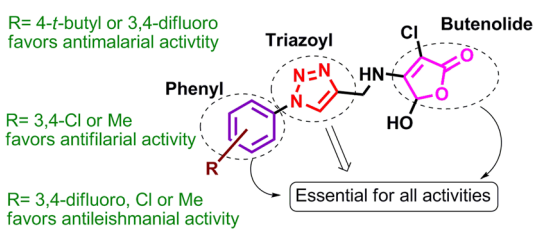

Fig. 2 Structure–activity relationship (SAR) predictions for the synthesized 1,2,3-triazole–butenolide conjugates.

***In vitro* and *in vivo* pharmacokinetic studies.** Further, to corroborate the results of the *in silico* ADME study of the synthesized series, we subjected compound **10u** to *in vitro* and *in vivo* pharmacokinetic studies. It was tested in microenvironments with varied pH, where it showed a satisfactory stability profile in simulated gastric fluid (SGF, pH 1.2), intestinal fluid (SIF, pH 6.8), and physiological fluid (SPF, pH 7.4), and *in vitro* plasma exposure. The percent analyte remaining after exposure to SGF, SIF, SPF, and plasma was found to be ≥70%, which indicates reasonable stability of the analyte under all the *in vitro* circumstances when observed for

Table 3 *In silico* ADME parameters important for good oral bioavailability of the synthesized compounds **10a–10w** and **11a**

Entry	% ABS	TPSA (Å^2)	n-ROTB[a]	MV	MW	miLogP	n-ON acceptors[b]	n-OHNH donors[c]	Lipinski's violation
Rule	—	—	—	—	<500	≤5	<10	<5	≤1
10a	75.43	98.51	5	270.18	336.74	1.01	8	2	0
10b	78.19	89.28	4	244.63	306.71	0.95	7	2	0
10c	78.19	89.28	4	261.20	320.74	1.40	7	2	0
10d	78.19	89.28	5	278.00	334.76	1.87	7	2	0
10e	78.19	89.28	4	258.17	341.15	1.63	7	2	0
10f	78.19	89.28	4	249.57	324.70	1.12	7	2	0
10g	78.19	89.28	5	310.82	362.82	2.66	7	2	0
10h	78.19	89.28	4	294.32	348.79	2.58	7	2	0
10i	71.82	107.75	6	295.73	366.76	0.81	9	2	0
10j	78.19	89.28	5	294.58	348.79	2.46	7	2	0
10k	78.19	89.28	4	277.76	334.76	2.20	7	2	0
10l	78.19	89.28	5	280.86	392.70	2.15	7	2	0
10m	78.19	89.28	4	271.71	375.60	2.45	7	2	0
10n	78.19	89.28	4	263.10	359.14	1.93	7	2	0
10o	78.19	89.28	5	275.93	374.71	2.04	7	2	0
10p	71.8	107.75	4	268.56	350.72	1.05	9	2	0
10q	78.19	89.28	7	311.60	362.82	2.82	7	2	0
10r	62.39	135.10	5	267.97	351.71	1.08	10	2	0
10s	68.88	116.28	7	321.27	396.79	1.01	10	2	0
10t	78.19	89.28	4	277.76	334.76	1.99	7	2	0
10u	78.19	89.28	4	254.50	342.69	1.42	7	2	0
10v	75.01	98.51	6	325.03	398.81	2.87	8	2	0
10w	78.19	89.28	4	266.13	338.73	1.71	7	2	0
11a	88.79	58.56	2	147.02	187.58	0.28	4	2	0

[a] n-ROTB – number of rotatable bonds. [b] n-ON acceptors – number of hydrogen bond acceptors. [c] n-OHNH donors – number of hydrogen bond donor.

120 min (Fig. 3A). Additionally, to confirm the *in vitro* results, an *in vivo* oral pharmacokinetic study of **10u** was performed in male golden hamsters at an active dose of 50 mg kg^{-1}. Fig. 3B shows a plot of the mean plasma drug concentration (log) of the analyte against time after oral delivery.

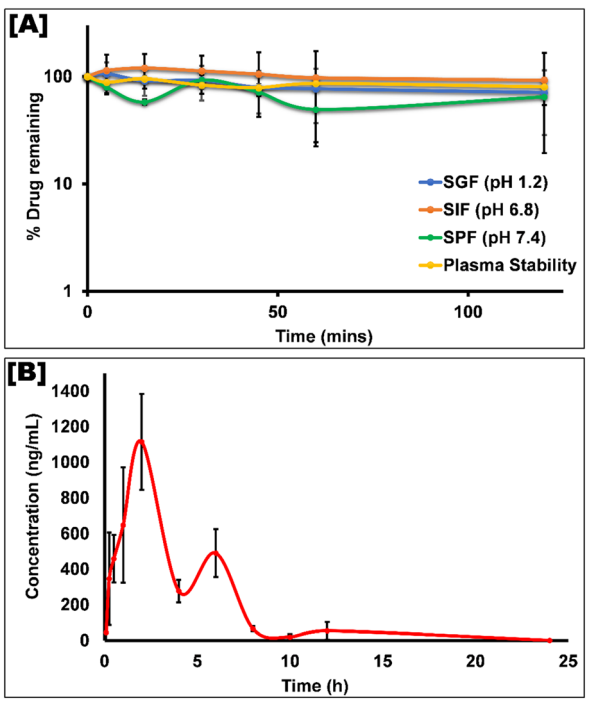

Fig. 3 (A) *In vitro* stability profile of **10u** at different simulated physiological microenvironments, whereas (B) represents the *in vivo* pharmacokinetic profile post oral administration of **10u** to experimental hamsters at a dose of 50 mg kg^{-1}.

Based on the *in vivo* pharmacokinetic profile of **10u**, the pharmacokinetic parameters were derived by applying non-compartmental analysis using Phoenix WinNonlin software. It was observed that after oral dosing, the analyte showed good absorption and permeation into the systemic circulation, exhibiting its C_{max} at 1114.94 ± 324.29 ng mL^{-1} within 2 h (T_{max}). From the pharmacokinetic profile, it was understood that **10u** follows enterohepatic recirculation with a half-life ($t_{1/2}$) of 2.15 ± 0.46 h and a total systemic residence time of 3.64 ± 0.23 h. The rate of elimination and distribution profile of the analyte was decent and can be seen in Table 4. Thus, it can be concluded that the candidate's oral pharmacokinetic profile is acceptable and can serve as proof for the candidate in further drug discovery optimizations.

Table 4 The estimated pharmacokinetic parameters of **10u** after oral administration in experimental hamsters. (n = 6)

Parameters	Unit	**10u**
C_{max}	ng mL^{-1}	1114.94 ± 324.29
T_{max}	h	2
AUC	h ng mL^{-1}	4501.64 ± 1358.92
$t_{1/2}$	h	2.15 ± 0.46
Cl	L h^{-1} kg^{-1}	12.39 ± 2.68
V_d	L kg^{-1}	38.15 ± 11.10
MRT	h	3.64 ± 0.23

C_{max}, maximum concentration at T_{max} (maximum time); AUC, area under the curve; $t_{1/2}$, half-life; Cl, clearance; V_d, apparent volume of distribution; MRT, mean residence time.

Conclusion

In the present study, 23 novel triazole–butenolide conjugates were designed and synthesized for evaluation against parasite-borne diseases. The results of the *in vitro* analysis proclaimed that these conjugates provided a step forward towards the discovery of new biodynamic agents. The structure–activity relationship (SAR) analysis, *in silico* ADME study and pharmacokinetic studies provided support and evidence that warrant further investigation and development of the conjugates as antiparasitic agents.

Experimental section

General chemistry

Reagents obtained from commercial sources were used without further purification. 100–200 mesh silica gel was used in column chromatography for the purification of compounds. The pace of chemical reactions was monitored by TLC (silica gel plates with fluorescence F254). Melting points were uncorrected. ^{1}H and ^{13}C NMR spectra were recorded at 400 MHz and 100 MHz, respectively, using $CDCl_3$ and DMSO-d_6 as a solvent. All chemical shift values are described in ppm and their multiplicities expressed as m = multiplet, q = quartet, t = triplet, dd = double doublet, brd = broad doublet, d = doublet, brs = broad singlet, and s = singlet. The ESI-MS spectra were recorded on an ion trap LCQ Advantage Max mass spectrometer (Thermo Electron Corporation) and HRMS spectra were recorded using a Q-TOF instrument (Agilent 6520). All the final compounds were found to be >95% pure as determined using an Agilent HPLC equipped with an Eclipse Plus C18 column (4.6 × 250 mm, 5 μm mesh size), with acetonitrile (solvent A) and water (solvent B) as an eluent in the ratio 9 : 1, at a flow rate of 0.80 ml min^{-1} and run time of 10 min. Detection was done by UV at 220 and 254 nm.

Synthesis of TBDMS *O*-protected mucochloric acid (7a)

To a well-stirred solution of mucochloric acid (1 mmol) in dichloromethane, 2,6-lutidine (2 mmol) was added followed by slow addition of TBDMSOTf (1.2 mmol). The reaction mixture was stirred for 1 h at room temperature. On completion of the reaction as monitored by thin layer chromatography, it was then quenched with an aqueous solution of sodium bicarbonate ($NaHCO_3$) followed by extraction with ethyl acetate. The organic layer was then washed with an aqueous solution of copper sulphate ($CuSO_4$) multiple times for the removal of remaining 2,6-lutidine from the reaction mixture. The combined organic layers were then dried over sodium sulphate (Na_2SO_4) and concentrated under a high vacuum. The obtained TBDMS *O*-protected mucochloric acid derivative was subjected to normal phase column chromatography and purified using 10% ethyl acetate : hexane as an eluent to afford a white crystalline solid product.

5-((*tert*-Butyldimethylsilyl)oxy)-3,4-dichlorofuran-2(5*H*)-one (7a). White solid; yield: 85%; ^{1}H NMR (400 MHz, DMSO-d_6): δ_H 0.19 (s, 3H), 0.22 (s, 3H), 0.91 (s, 9H), 6.40 (s, 1H); ^{13}C NMR (100 MHz, DMSO-d_6): δ_C −5.3, −4.9, 17.6, 25.2, 96.4, 121.6, 150.4, 163.0.

Synthesis of propargyl amine substituted *O*-protected mucochloric acid (8a)

The TBDMS *O*-protected mucochloric acid derivative (1 mmol) **7a** obtained in the first step was then dissolved in DMF followed by addition of propargyl amine (1.5 mmol). The reaction was then allowed to stir at room temperature for 1 h. On consumption of the starting material as monitored by TLC, the reaction mixture was then poured over crushed ice followed by continuous trituration, and then extraction was done with ethyl acetate. The obtained combined organic layer was then dried over Na_2SO_4 and concentrated under a high vacuum. Further purification was carried out *via* normal phase chromatography using 20% ethyl acetate : hexane as an eluting solvent to afford propargyl amine substituted *O*-protected mucochloric acid as a white amorphous solid in pure form.

5-((*tert*-Butyldimethylsilyl)oxy)-3-chloro-4-(prop-2-yn-1-ylamino)furan-2(5*H*)-one (8a). White solid; yield: 88%; ^{1}H NMR (400 MHz, DMSO-d_6): δ_H 0.17 (s, 3H), 0.19 (s, 3H), 0.89 (s, 9H), 3.35 (t, 1H), 4.12 (S, 2H), 6.24 (brs, 1H), 8.05 (s, 1H); ^{13}C NMR (100 MHz, $CDCl_3$): δ_C −4.8, −4.1, 17.9, 25.6, 33.3, 73.7, 78.7, 92.8, 158.1, 167.0.

General synthesis of 1,2,3-triazole containing *O*-protected butenolide conjugates (9a–9w)

Alkyne (1 mmol) **8a** thus obtained in the second step and different substituted aromatic azides were then suspended in DMF. To the stirred mixture of alkyne and azide, sodium ascorbate (0.3 mmol) was added followed by addition of copper sulphate pentahydrate ($CuSO_4{\cdot}5H_2O$) (0.03 mmol). This reaction mixture was then stirred at 60 °C for 1 h. On completion of the reaction, the mixture was diluted with ice water followed by extraction with ethyl acetate. The obtained organic layer was then dried over Na_2SO_4 and concentrated under a high vacuum followed by purification *via* normal phase chromatography using 20% ethyl acetate : hexane as an eluent to afford the respective 1,2,3-triazole containing *O*-protected butenolide conjugates **9a–9w** in pure form.

5-((*tert*-Butyldimethylsilyl)oxy)-3-chloro-4-(((1-mesityl-1*H*-1,2,3-triazol-4-yl)methyl)amino)furan-2(5*H*)-one (9h). White solid; yield: 85%; ^{1}H NMR (400 MHz, $CDCl_3$): δ_H 0.19 (s, 3H), 0.21 (s, 3H), 0.90 (s, 9H), 1.93 (s, 6H), 2.35 (s, 3H), 4.85–4.96 (m, 2H), 5.61 (brs, 1H), 6.03 (brs, 1H), 6.99 (s, 2H), 7.59 (s, 1H); ^{13}C NMR (100 MHz, $CDCl_3$): δ_C -4.7, −4.0, 17.4, 17.9, 21.2, 25.7, 39.0, 88.1, 93.2, 123.8, 129.3, 133.3, 135.0, 140.5, 143.8, 158.0, 167.3.

General synthesis of 1,2,3-triazole–butenolide conjugates (10a–10w)

For the removal of the *tert*-butyldimethylsilyl group, tetra-*n*-butylammonium fluoride (TBAF) (1.0 M solution in THF, 0.55 mmol) was added to a stirred solution of 1,2,3-triazole containing *O*-TBDMS-protected butenolide conjugates in dry DMF at −30 °C followed by further stirring of the reaction mixture at the same temperature for 1 h. On completion, the

reaction mixture was quenched with aqueous 3% hydrochloric acid solution followed by extraction with ethyl acetate. The organic layer was washed with brine solution, dried over Na_2SO_4 and evaporated under a high vacuum to obtain the crude mixture, which was then washed with a mixture of ether and hexane (1 : 1) to afford deprotected 1,2,3-triazole–butenolide conjugates as a yellow solid in pure form.

3-Chloro-5-hydroxy-4-(((1-(4-methoxyphenyl)-1*H*-1,2,3-triazol-4-yl)methyl)amino)furan-2(5*H*)-one (10a). Yellow solid; yield: 85%; mp: 159–161 °C; ^{1}H NMR (400 MHz, DMSO-d_6): δ_H 3.83 (s, 3H), 4.64–4.73 (m, 2H), 6.21 (brs, 1H), 7.14 (d, J = 8.7 Hz, 2H), 7.79 (d, J = 8.7 Hz, 2H), 8.58 (brs, 1H), 8.08 (brs, 1H), 8.14 (s, 1H); ^{13}C NMR (100 MHz, DMSO-d_6): δ_C 38.2, 55.6, 92.5, 114.9, 121.3, 121.7, 130.0, 145.6, 159.3, 167.0; HRMS (ESI) m/z 337.0696 $[M + H]^+$ (calcd. for $C_{14}H_{14}ClN_4O_4$, 337.0704).

3-Chloro-5-hydroxy-4-(((1-phenyl-1*H*-1,2,3-triazol-4-yl)methyl)amino)furan-2(5*H*)-one (10b). Yellow solid; yield: 80%; mp: 171–173 °C; ^{1}H NMR (400 MHz, DMSO-d_6): δ_H 4.74 (s, 2H), 6.17 (brs, 1H), 7.48–7.52 (m, 2H), 7.58–7.62 (m, 1H), 7.87–7.90 (m, 2H), 8.17 (brs, 2H), 8.70 (s, 1H); ^{13}C NMR (100 MHz, DMSO-d_6): δ_C 38.1, 84.3, 92.6, 120.0, 121.3, 128.7, 129.9, 136.6, 145.9, 160.0, 167.2; HRMS (ESI) m/z 307.0589 $[M + H]^+$ (calcd. for $C_{13}H_{12}ClN_4O_3$, 307.0598).

3-Chloro-5-hydroxy-4-(((1-(p-tolyl)-1*H*-1,2,3-triazol-4-yl)methyl)amino)furan-2(5*H*)-one (10c). Yellow solid; yield: 87%; mp: 134–136 °C; ^{1}H NMR (400 MHz, DMSO-d_6): δ_H 2.38 (s, 3H), 4.65–4.76 (m, 2H), 6.22 (brs, 1H), 7.40 (d, J = 8.2 Hz, 2H,), 7.77 (d, J = 8.4 Hz, 2H), 8.64 (brs, 1H), 8.08 (brs, 1H), 8.15 (s, 1H); ^{13}C NMR (100 MHz, DMSO-d_6): δ_C 20.6, 38.2, 84.3, 92.5, 119.9, 121.2, 130.2, 134.4, 138.3, 145.7, 160.0, 167.2; HRMS (ESI) m/z 321.0746 $[M + H]^+$ (calcd. for $C_{14}H_{14}ClN_4O_3$, 321.0754).

3-Chloro-4-(((1-(4-ethylphenyl)-1*H*-1,2,3-triazol-4-yl)methyl)amino)-5-hydroxyfuran-2(5*H*)-one (10d). Off-white solid; yield: 82%; mp: 145–147 °C; ^{1}H NMR (400 MHz, DMSO-d_6): δ_H 1.22 (t, J = 7.5 Hz, 3H), 2.68 (q, J = 7.5 Hz, 15.0 Hz, 2H), 4.64–4.74 (m, 2H), 6.20 (brs, 1H), 7.43 (d, J = 8.3 Hz, 2H), 7.78 (d, J = 8.3 Hz, 2H,), 8.64 (brs, 1H), 8.08 (brs, 1H), 8.15 (s, 1H); ^{13}C NMR (100 MHz, DMSO-d_6): δ_C 15.4, 27.7, 38.2, 92.5, 120.0, 121.2, 129.1, 134.6, 144.5, 145.7, 167.2; HRMS (ESI) m/z 335.0904 $[M + H]^+$ (calcd. for $C_{15}H_{16}ClN_4O_3$, 335.0911).

3-Chloro-4-(((1-(4-chlorophenyl)-1*H*-1,2,3-triazol-4-yl)methyl)amino)-5-hydroxyfuran-2(5*H*)-one (10e). Off-white solid; yield: 89%; mp: 172–174 °C; ^{1}H NMR (400 MHz, DMSO-d_6): δ_H 4.58–4.76 (m, 2H), 6.19 (brs, 1H), 7.68 (d, J = 8.8 Hz, 2H), 7.94 (d, J = 8.8 Hz, 2H), 8.09 (brs, 1H), 8.16 (brs, 1H), 8.72 (s, 1H); ^{13}C NMR (100 MHz, DMSO-d_6): δ_C 38.2, 92.6, 121.4, 121.7, 129.9, 133.0, 135.4, 146.1, 167.1; HRMS (ESI) m/z 341.0199 $[M + H]^+$ (calcd. for $C_{13}H_{11}Cl_2N_4O_3$, 341.0208).

3-Chloro-4-(((1-(4-fluorophenyl)-1*H*-1,2,3-triazol-4-yl)methyl)amino)-5-hydroxyfuran-2(5*H*)-one (10f). Yellow solid; yield: 85%; mp: 146–148 °C; ^{1}H NMR (400 MHz, DMSO-d_6): δ_H 4.58–4.78 (m, 2H), 6.17 (brs, 1H), 7.44–7.48 (m, 2H), 7.92–7.96 (m, 2H), 8.08 (brs, 1H), 8.16 (brs, 1H), 8.67 (s, 1H); ^{13}C NMR (100 MHz, DMSO-d_6): δ_C 38.1, 92.5, 116.6, 116.9, 121.6, 122.3, 122.4, 133.2, 145.9, 160.4, 162.8; HRMS (ESI) m/z 325.0496 $[M+H]^+$ (calcd. for $C_{13}H_{11}ClFN_4O_3$, 325.0504).

4-(((1-(4-(*tert*-Butyl)phenyl)-1*H*-1,2,3-triazol-4-yl)methyl)amino)-3-chloro-5-hydroxyfuran-2(5*H*)-one (10g). Light brown solid; yield: 88%; mp: 145–147 °C; ^{1}H NMR (400 MHz, DMSO-d_6): δ_H 1.33 (s, 9H), 4.73–4.76 (m, 2H), 6.20 (brs, 1H), 7.59–7.62 (m, 2H), 7.77–7.80 (m, 2H), 8.09 (brs, 1H), 8.15 (brs, 1H), 8.64 (s, 1H); ^{13}C NMR (100 MHz, DMSO-d_6): δ_C 31.01, 34.5, 38.2, 92.6, 119.8, 121.3, 126.6, 134.3, 145.7, 151.4; HRMS (ESI) m/z 363.1217 $[M + H]^+$ (calcd. for $C_{17}H_{20}ClN_4O_3$, 363.1224).

3-Chloro-5-hydroxy-4-(((1-mesityl-1*H*-1,2,3-triazol-4-yl)methyl)amino)furan-2(5*H*)-one (10h). Yellow solid; yield: 90%; mp: 79–81 °C; ^{1}H NMR (400 MHz, $CDCl_3$): δ_H 1.89 (s, 6H), 2.34 (s, 3H), 4.91–4.494 (m, 2H), 6.09 (brs, 1H), 6.27 (s, 1H), 6.95 (s, 2H), 7.68 (s, 1H); ^{13}C NMR (100 MHz, $CDCl_3$): δ_C 17.2, 21.2, 38.7, 86.6, 93.3, 124.8, 129.2, 133.1, 134.9, 140.3, 144.5, 158.6, 169.1; HRMS (ESI) m/z 349.1058 $[M + H]^+$ (calcd. for $C_{16}H_{18}ClN_4O_3$, 349.1067).

3-Chloro-4-(((1-(3,4-dimethoxyphenyl)-1*H*-1,2,3-triazol-4-yl)methyl)amino)-5-hydroxyfuran-2(5*H*)-one (10i). Brown solid; yield: 89%; mp: 167–169 °C; ^{1}H NMR (400 MHz, DMSO-d_6): δ_H 3.82 (s, 3H), 3.86 (s, 3H), 4.71 (brs, 2H), 6.13–6.15 (brs, 1H), 7.13 (d, J = 8.8 Hz, 1H), 7.39 (dd, J = 2.6 Hz, 8.6 Hz, 1H), 7.44 (d, J = 2.5 Hz, 1H), 8.20 (brs, 1H), 8.66 (s, 1H); ^{13}C NMR (100 MHz, DMSO-d_6): δ_C 38.6, 56.3, 93.1, 105.1, 112.5, 112.6, 122.0, 130.6, 146.0, 149.4, 149.8. HRMS (ESI) m/z 367.0800[M + H]$^+$ (calcd. for $C_{15}H_{16}ClN_4O_5$ 367.0809).

3-Chloro-5-hydroxy-4-(((1-(4-isopropylphenyl)-1*H*-1,2,3-triazol-4-yl)methyl)amino)furan-2(5*H*)-one (10j). Off-white solid; yield: 85%; mp: 151–153 °C; ^{1}H NMR (400 MHz, DMSO-d_6): δ_H 1.24 (d, J = 6.9 Hz, 6H), 2.94–3.01 (m, 1H), 4.64–4.77 (m, 2H), 6.19 (brs, 1H), 7.46 (d, J = 8.5 Hz, 2H), 7.79 (d, J = 8.7 Hz, 2H), 8.08 (brs, 1H), 8.16 (brs, 1H), 8.63 (s, 1H); ^{13}C NMR (100 MHz, DMSO-d_6): δ_C 23.7, 33.0, 38.1, 84.0, 92.5, 120.1, 121.2, 127.7, 134.6, 145.7, 149.1, 167.2; HRMS (ESI) m/z 349.1058 $[M + H]^+$ (calcd. for $C_{16}H_{18}ClN_4O_3$, 349.1067).

3-Chloro-4-(((1-(2,5-dimethylphenyl)-1*H*-1,2,3-triazol-4-yl)methyl)amino)-5-hydroxyfuran-2(5*H*)-one (10k). Brown solid; yield: 83%; mp: 96–98 °C; ^{1}H NMR (400 MHz, DMSO-d_6): δ_H 2.10 (s, 3H), 2.35 (s, 1H), 4.74–4.75 (m, 2H), 6.17 (brs, 1H), 7.23 (s, 1H), 7.30 (d, J = 8.0 Hz, 1H), 7.35 (d, J = 7.8 Hz, 1H), 8.08 (brs, 1H), 8.16 (brs, 1H), 8.33 (s, 1H); ^{13}C NMR (100 MHz, DMSO-d_6): δ_C 17.0, 20.2, 38.1, 84.3, 92.6, 124.6, 126.2, 129.7, 130.4, 131.2, 136.1, 136.5, 144.8, 167.3; HRMS (ESI) m/z 335.0904 $[M + H]^+$ (calcd. for $C_{15}H_{16}ClN_4O_3$, 335.0911).

3-Chloro-4-(((1-(4-fluoro-3-(trifluoromethyl)phenyl)-1*H*-1,2,3-triazol-4-yl)methyl)amino)-5-hydroxyfuran-2(5*H*)-one (10l). Off-white solid; yield: 91%; mp: 123–125 °C; ^{1}H NMR (400 MHz, DMSO-d_6): δ_H 3.83 (s, 3H), 4.64–4.73 (2H, m), 6.21 (1H, brs), 7.14 (d, J = 8.7 Hz, 2H), 7.79 (d, J = 8.7 Hz, 2H), 8.58 (brs, 1H), 8.08 (brs, 1H), 8.14 (s, 1H); ^{13}C NMR (100 MHz, DMSO-d_6): δ_C 38.1, 92.4, 118.0, 120.7, 120.8, 120.9, 120.9, 121.7, 122.3, 133.6, 133.6, 146.1, 155.6, 158.1, 167.1; HRMS (ESI) m/z 393.9935 $[M + H]^+$ (calcd. for $C_{14}H_{10}ClF_4N_4O_4$, 393.0378).

3-Chloro-4-(((1-(3,4-dichlorophenyl)-1*H*-1,2,3-triazol-4-yl)-methyl)amino)-5-hydroxyfuran-2(5*H*)-one (10m). Yellow solid; yield: 85%; mp: 161–163 °C; ^{1}H NMR (400 MHz, DMSO-d_6): δ_H 4.73–4.78 (m, 2H), 6.16 (brs, 1H), 7.87–7.89 (m, 1H), 7.95–7.98 (m, 1H), 8.08 (brs, 1H), 8.17 (brs, 1H), 8.25–8.26 (m, 1H), 8.80 (s, 1H); ^{13}C NMR (100 MHz, DMSO-d_6): δ_C 38.1, 92.5, 120.0, 121.5, 121.7, 131.0, 131.8, 132.4, 136.1, 146.2, 167.0; HRMS (ESI) *m*/*z* 374.9813 $[M + H]^+$ (calcd. for $C_{13}H_{10}Cl_3N_4O_3$, 374.9818).

3-Chloro-4-(((1-(3-chloro-4-fluorophenyl)-1*H*-1,2,3-triazol-4-yl)methyl)amino)-5-hydroxyfuran-2(5*H*)-one (10n). Yellow solid; yield: 88%; mp: 133–135 °C; ^{1}H NMR (400 MHz, DMSO-d_6): δ_H 4.66–4.79 (m, 2H), 6.17 (brs, 1H), 7.80 (t, *J* = 9.8 Hz, 1H), 8.09–8.11 (m, 1H), 8.18 (brs, 1H), 8.27–8.33 (m, 2H), 8.84 (s, 1H); ^{13}C NMR (100 MHz, DMSO-d_6): δ_C 38.1, 84.3, 92.5, 117.5, 117.7, 117.8, 118.0, 118.3, 119.0, 119.2, 120.7, 121.9, 123.4, 126.1, 126.9, 127.0, 133.2, 146.2, 156.9, 159.9, 159.4, 167.1; HRMS (ESI) *m*/*z* 377.0234 $[M + NH_4]^+$ (calcd. for $C_{13}H_{15}Cl_2N_5O_4$, 377.0220).

3-Chloro-5-hydroxy-4-(((1-(3-(trifluoromethyl)phenyl)-1*H*-1,2,3-triazol-4-yl)methyl)amino)furan-2(5*H*)-one (10o). Off-white solid; yield: 87%; mp: 141–143 °C; ^{1}H NMR (400 MHz, DMSO-d_6): δ_H 4.67–4.80 (m, 2H), 6.20 (brs, 1H), 7.83–7.89 (m, 2H), 8.09–8.11 (m, 1H), 8.18 (brs, 1H), 8.23–8.27 (m, 2H), 8.88 (s, 1H); ^{13}C NMR (100 MHz, DMSO-d_6): δ_C 38.1, 84.2, 92.5, 116.6, 116.6, 119.5, 121.7, 122.2, 124.0, 124.9, 125.2, 125.2, 127.6, 130.1, 130.4, 130.7, 131.1, 137.1, 146.2, 167.1; HRMS (ESI) *m*/*z* 375.0465 $[M + H]^+$ (calcd. for $C_{14}H_{11}ClF_3N_4O_3$, 375.0472).

4-(((1-(Benzo[*d*][1,3]dioxol-5-yl)-1*H*-1,2,3-triazol-4-yl)-methyl)amino)-3-chloro-5-hydroxyfuran-2(5*H*)-one (10p). Off-white semi-solid; yield: 78%; ^{1}H NMR (400 MHz, DMSO-d_6): δ_H 4.61–4.78 (m, 2H), 6.15 (brs, 1H), 6.36 (s, 2H), 7.44 (s, 1H), 7.85 (s, 1H), 8.11 (brs, 1H), 8.20 (brs, 1H), 8.46 (s, 1H); ^{13}C NMR (100 MHz, DMSO-d_6): δ_C 38.4, 104.9, 106.0, 108.0, 125.2, 125.9, 139.2, 149.1, 152.0; HRMS (ESI) *m*/*z* 351.0487 $[M + H]^+$ (calcd. for $C_{14}H_{12}ClN_4O_5$, 351.0496).

4-(((1-(4-Butylphenyl)-1*H*-1,2,3-triazol-4-yl)methyl)amino)-3-chloro-5-hydroxyfuran-2(5*H*)-one (10q). Yellow solid; yield: 89%; mp: 149–151 °C; ^{1}H NMR (400 MHz, DMSO-d_6): δ_H 0.91 (t, *J* = 7.3 Hz, 3H), 1.28–1.41 (m, 2H), 1.55–1.63 (m, 2H), 2.66 (t, *J* = 7.6 Hz, 2H), 4.64–4.76 (m, 2H), 6.19 (brs, 1H), 7.41 (d, *J* = 8.4 Hz, 2H), 7.77 (d, *J* = 8.6 Hz, 2H), 8.08 (brs, 1H), 8.15 (brs, 1H), 8.63 (s, 1H); ^{13}C NMR (100 MHz, DMSO-d_6): δ_C 13.7, 21.7, 32.9, 34.2, 38.1, 92.5, 120.0, 129.6, 134.5, 143.1, 167.1; HRMS (ESI) *m*/*z* 363.1217 $[M + H]^+$ (calcd. for $C_{17}H_{20}ClN_4O_3$, 363.1224).

3-Chloro-5-hydroxy-4-(((1-(2-nitrophenyl)-1*H*-1,2,3-triazol-4-yl)methyl)amino)furan-2(5*H*)-one (10r). Brown semi-solid; yield: 83%; ^{1}H NMR (400 MHz, DMSO-d_6): δ_H 4.67–4.80 (m, 2H), 6.13 (brs, 1H), 7.82–7.86 (m, 2H), 7.94–7.98 (m, 1H), 8.11 (brs, 1H), 8.21–8.23 (m, 2H), 8.60 (s, 1H); ^{13}C NMR (100 MHz, DMSO-d_6): δ_C 38.0, 92.6, 124.4, 125.5, 127.5, 129.1, 131.2, 134.4, 144.0, 145.6, 167.1; HRMS (ESI) *m*/*z* 352.0432 $[M + H]^+$ (calcd. for $C_{13}H_{11}ClN_5O_5$, 352.0449).

3-Chloro-5-hydroxy-4-(((1-(3,4,5-trimethoxyphenyl)-1*H*-1,2,3-triazol-4-yl)methyl)amino)furan-2(5*H*)-one (10s). White solid; yield: 88%; mp: 144–146 °C; ^{1}H NMR (400 MHz, DMSO-d_6): δ_H 3.71 (s, 3H), 3.88 (s, 6H), 4.66–4.78 (m, 2H), 6.18 (brs, 1H), 7.17 (s, 2H), 8.12–8.17 (m, 2H), 8.70 (s, 1H); ^{13}C NMR (100 MHz, DMSO-d_6): δ_C 38.2, 56.3, 60.2, 84.2, 92.5, 98.2, 121.6, 132.5, 137.4, 145.5, 153.5, 167.1; HRMS (ESI) *m*/*z* 397.0903 $[M + H]^+$ (calcd. for $C_{16}H_{18}ClN_4O_6$, 397.0915).

3-Chloro-4-(((1-(3,4-dimethylphenyl)-1*H*-1,2,3-triazol-4-yl)-methyl)amino)-5-hydroxyfuran-2(5*H*)-one (10t). Yellow solid; yield: 86%; mp: 156–158 °C; ^{1}H NMR (400 MHz, DMSO-d_6): δ_H 2.28 (s, 3H), 2.32 (s, 3H), 4.66–4.73 (m, 2H), 6.21 (brs, 1H), 7.34 (d, *J* = 8.2 Hz, 1H), 7.58 (dd, *J* = 1.9 Hz, 8.1 Hz, 1H), 7.68 (s, 1H), 8.08 (brs, 1H), 8.15 (brs, 1H), 8.61 (s, 1H); ^{13}C NMR (100 MHz, DMSO-d_6): δ_C 18.9, 19.4, 38.2, 92.6, 117.2, 120.8, 121.1, 130.6, 134.5, 137.0, 138.1, 145.7, 160.0, 167.0; HRMS (ESI) *m*/*z* 335.0899 $[M + H]^+$ (calcd. for $C_{15}H_{16}ClN_4O_3$, 335.0911).

3-Chloro-4-(((1-(3,4-difluorophenyl)-1*H*-1,2,3-triazol-4-yl)-methyl)amino)-5-hydroxyfuran-2(5*H*)-one (10u). Brown solid; yield: 92%; mp: 111–113 °C; ^{1}H NMR (400 MHz, DMSO-d_6): δ_H 4.75 (s, 2H), 6.16 (brs, 1H), 7.33–7.38 (m, 1H), 7.66–7.71 (m, 1H), 7.86–7.92 (m, 1H), 8.11 (brs, 1H), 8.17 (brs, 1H), 8.48–8.49 (m, 1H); ^{13}C NMR (100 MHz, DMSO-d_6): δ_C38.0, 92.6, 105.5, 105.7, 106.0, 112.6, 112.9, 113.9, 121.7, 121.7, 124.8, 127.4, 127.5, 127.6, 145.3, 153.1, 153.2, 155.6, 155.7, 160.9, 161.0, 163.3, 163.5, 167.0; HRMS (ESI) *m*/*z* 343.0405 $[M + H]^+$ (calcd. for $C_{13}H_{10}ClF_2N_4O_3$, 343.0409).

3-Chloro-5-hydroxy-4-(((1-(2-phenoxyphenyl)-1*H*-1,2,3-triazol-4-yl)methyl)amino)furan-2(5*H*)-one (10v). Off-white solid; yield: 87%; mp: 136–138 °C; ^{1}H NMR (400 MHz, $CDCl_3$): δ_H 4.82–4.84 (m, 2H), 6.00 (brs, 1H), 6.93–7.09 (m, 2H), 7.11–7.23 (m, 1H), 7.25–7.30 (m, 1H), 7.32–7.37 (m, 1H), 7.36–7.37 (m, 2H), 7.39–7.41 (m, 1H), 7.41 (s, 1H); ^{13}C NMR (100 MHz, $CDCl_3$): δ_C 87.1, 93.2, 118.8, 119.8, 124.5, 124.6, 125.9, 128.1, 130.2, 130.7, 144.1, 148.9, 155.7, 168.8; HRMS (ESI) *m*/*z* 399.0843 $[M + H]^+$ (calcd. for $C_{19}H_{16}ClN_4O_4$, 399.0860).

3-Chloro-4-(((1-(3-fluoro-4-methylphenyl)-1*H*-1,2,3-triazol-4-yl)methyl)amino)-5-hydroxyfuran-2(5*H*)-one (10w). Off-white solid; yield: 78%; mp: 152–154 °C; ^{1}H NMR (400 MHz, DMSO-d_6): δ_H 2.40 (s, 3H), 4.65–4.74 (m, 2H), 6.17 (brs, 1H), 7.58 (d, *J* = 8.5 Hz, 1H), 7.82 (dd, *J* = 2.3 Hz, 8.3 Hz, 1H), 8.01 (d, *J* = 2.2 Hz, 1H), 8.08 (brs, 1H), 8.16 (brs, 1H), 8.74 (s, 1H); ^{13}C NMR (100 MHz, DMSO-d_6): δ_C 19.2, 38.1, 92.6, 118.5, 120.0, 121.3, 132.3, 134.2, 135.5, 136.0, 146.0, 167.2; HRMS (ESI) *m*/*z* 339.0217 $[M + H]^+$ (calcd. for $C_{14}H_{13}ClFN_4O_3$, 339.0660).

Synthesis of propargyl amine substituted-butenolide conjugate (11a)

8a was subjected to the same procedure of deprotection as for the synthesis of **10a–10w** derivatives.

3-Chloro-5-hydroxy-4-(prop-2-yn-1-ylamino)furan-2(5*H*)-one (11a). Off-white solid; yield: 90%; mp: 87–89 °C; ^{1}H NMR (400 MHz, DMSO-d_6): δ_H 3.32 (t, *J* = 2.5 Hz, 1H), 4.14–4.19 (m, 2H), 6.01 (brs, 1H), 8.01 (t, *J* = 6.1 Hz, 1H), 8.11 (d, *J* = 8.5 Hz,

1H); ^{13}C NMR (100 MHz, DMSO-d_6): δ_C 32.1, 38.9, 74.9, 80.5, 84.7, 92.4, 159.1, 159.5, 167.1; HRMS (ESI) m/z 188.0105 $[M + H]^+$ (calcd. for $C_7H_7ClNO_3$, 188.0114).

Biological evaluation

Parasite

L. donovani (WHO designation MHOM/IN/80/Dd8, received as a gift through the kind courtesy of the late Prof. P. C. C. Garnham from Imperial College, London) were transfected with luciferase reporter gene[14] and used for *in vitro* evaluation of antileishmanial activity. The expression of transfectants was stable under the influence of G418 (20 μg ml^{-1}). These transfectants were maintained in Medium 199 (Sigma Chemical Co., USA) at 25 ± 1 °C supplemented with 10% heat-inactivated fetal calf serum (Gibco, Gaithersburg, MD) and 1% penicillin–streptomycin–amphotericin B suspension, 0.1 μM filtered, suitable for cell culture (Sigma Chemical Co., USA).

In vitro antileishmanial (anti-promastigote) activity

The effect of the compounds on the growth of promastigotes was assessed by monitoring the luciferase activity of viable cells after treatment with the compound. Transgenic promastigotes of late log phase were seeded at 5×10^5 cells per well in 96-well flat-bottomed microtitre (MT) plates (Cellstar, Greiner Bio-One GmbH, Monroe, NC) and were incubated for 72 h in medium alone or in the presence of serial dilutions of antileishmanial agents in DMSO. Parallel dilutions of DMSO were used as controls. After incubation, an aliquot (50 μl) of promastigote suspension was aspirated from each well and mixed with an equal volume of Steady-Glo reagent (Promega, Madison, WI), and the luminescence was measured using a luminometer. The values were expressed as relative luminescence unit (RLU). The inhibition of parasitic growth was determined by comparing the luciferase activity of drug-treated parasites with that of untreated controls using the formula:

$$\text{Percentage inhibition} = [N - n/N] \times 100$$

where N is the average relative luminescence unit (RLU) of control wells and n is the average RLU of treated wells.

In vitro antileishmanial (anti-amastigote) activity

To assess the *in vitro* antileishmanial activity of the compounds against the amastigote stage of the parasite, a mouse macrophage cell line (J-774A.1; obtained from NCCS, Pune) infected with promastigotes expressing luciferase firefly reporter gene were used. The J774A cells were seeded in a 96-well plate (2×10^5 cells per 200 μl per well) in RPMI-1640 containing 15% fetal calf serum and 1% antibiotic and antimycotic solution. The plates were incubated at 37 °C in a CO_2 incubator. After 24 h, the medium was replaced with fresh medium containing stationary phase promastigotes (2×10^6 per 200 μl per well). Promastigotes are internalized into the macrophage and are transformed into amastigotes. The test material in appropriate concentrations in complete medium was added after replacing the previous medium and the plates were incubated at 37 °C in a CO_2 incubator for 48 h. After incubation, the drug containing medium was decanted and 50 μl PBS was added in each well and mixed with an equal volume of Steady-Glo reagent. After gentle shaking for 1–2 min, the reading was taken using a luminometer. The values were expressed as relative luminescence unit (RLU). The inhibition of parasitic growth was determined as described above.

Cytotoxicity against the J774A cell line (MTT method)

J774A cells were seeded in a 96-well plate at a concentration of 0.2 million cells per well. The plates were incubated overnight in a CO_2 incubator with a supply of 5% CO_2 at 37 °C. Different concentrations of the test compounds and reference drugs dissolved in DMSO were added. Parallel dilutions of DMSO alone were used as controls. The plates were incubated further for 48 h and the number of viable cells per well was determined by the formation of a blue formazan product of MTT, generated as a result of mitochondrial dehydrogenase activity in viable cells.[19] The relative O.D. was measured at 600 nm against the blank using an automated microplate reader (SpectraMax, Molecular Devices). The cytotoxic effect was expressed as 50% lethal dose (CC_{50}), *i.e.*, concentration of a compound which provoked 50% reduction in cell viability compared to that of cells in culture medium alone. The results indicate percentage reductions in cell viability and were compared with those of untreated control wells.

Data analysis

The IC_{50} and CC_{50} values were calculated by regression obtained through probit analysis[14] of the log dose/response of the drug. The data were presented as mean ± standard deviation of three determinations from a minimum of at least three independent experiments. A p-value of <0.05 was considered significant.

In silico ADME study

In the present study, Molinspiration property engine v2022.08 (**https://www.molinspiration.com/cgi-bin/properties**) was employed to calculate all the molecular physicochemical properties of the synthesized compounds.[22]

Pharmacokinetic studies

LC-MS/MS conditions

The bioanalytical estimation of compound **10u** was carried out using a Shimadzu Nexera XS Series Liquid Chromatography and Mass Spectrometry System (LCMS-8050, Kyoto, Japan). In combination with a Waters Symmetry C18 analytical column (150 mm × 4.6 mm, 5 μ), an isocratic mobile phase consisting of acetonitrile (90%) and deionized water (10%) was used for chromatographic separation. The LC parameters like column oven temperature, injection volume, run time, autosampler temperature, and flow rate were kept at 40 °C, 20 μL, 5 min, 15 °C, and 0.7 mL min^{-1}, respectively. All of the MS settings for **10u** were fine-tuned to achieve a molecular mass of 374 Da at a high resolution. The required optimizations were carried out to identify the stable precursors (Q1) and product ions (Q3). In the continuous generation of Q3, argon acted as the collision gas. Carbamazepine (CBZ) served as the internal standard (IS) in this study. The software Shimadzu Lab Solutions was used for all aspects of the process, including operation, measurement, and analysis. Table 5 provides a tabular representation of the compounds' MS-dependent parameters.

In vitro and *in vivo* pharmacokinetics

The analyte was investigated to evaluate its pharmacokinetic profile using multiple *in vitro* and *in vivo* assays. The compound **10u** was examined *in vitro* under various microenvironments, such as SGF, SIF, SPF, and isolated hamster plasma. Internally, the artificially imitated solutions were developed in compliance with USP standards.[23] The simulated solutions and hamster plasma were pre-incubated at 37 ± 2 °C for 15 min in a shaking water bath (Julabo, Seelbach, Germany). At different time periods up to 120 min after each tube had been incubated and spiked with a specific amount of compound, a part of the fluids was collected post-spiking. The reaction was halted with the aid of 300 μL of LCMS-grade acetonitrile. The sample mixture was vigorously vortexed and centrifuged (at 14 000 rcf for 15 min) to deposit solid residues completely. 250 μL of the supernatant was then withdrawn for LC-MS analysis. The experiments were done three times to ensure accurate results.

Likewise, the *in vivo* pharmacokinetic fate of the analyte was examined by administering an oral suspension of **10u** at a dosage of 50 mg kg^{-1} to male golden hamsters (n = 6). Before the day of the experiment, the animals were allowed access to light and water but were required to abstain from food intake. After administration of the dose, blood was collected from the retroorbital plexus at specified intervals ranging from 5 min to 24 h. Before any blood was drawn from the animals, they were put under anesthesia. The blood-filled microcentrifuge tube was spun at a speed of 6000g for a period of 20 min so that the clear supernatant plasma could be extracted from it. After that, the plasma was stored in a refrigerator at a temperature of −80 °C until the conclusion of the analysis. The analyte was extracted using 200 μL of acetonitrile pre-mixed with IS at a concentration of 3 ng mL^{-1} using the standard protein precipitation method. The mixture was vortexed (5 min) and centrifuged at 12 000g for 20 min. 150 μL of supernatant liquid was withdrawn and subjected to LC-MS/MS analysis. The bioanalytical quantification and data analysis were done using LabSolutions software, whereas non-compartmental pharmacokinetic analysis (NCA) was performed using Phoenix WinNonlin software (Certara Inc., New Jersey, USA).[24] The graphical data were represented using GraphPad software, Inc. (San Diego, California, USA).

Animal ethics statement

The *in vivo* pharmacokinetics study was performed on experimental golden hamsters in accordance with the animal ethics guidelines and consent of the Institutional Animal

Table 5 Instrument, analyte, and IS-optimized MS parameters

Ion source parameters	Values
Interface temperature	350 °C
Heat block temperature	400 °C
Nebulizer gas	Nitrogen
Heating and drying gas	Nitrogen
Collision gas (CAD)	270 kPa
Voltage	5000 eV
Dwell time	100 ms
Polarity	Positive
Desolvation line temperature	250 °C
Quadrupole resolution	1

Analyte parameters	**10u**	CBZ (IS)
Q1/Q3, m/z	375.2/198.3	237.3/194.05
Q1 prebias	−30	−16
CE	−20	−21
Q3 prebias	−29	−23

Q1, precursor ion; Q3, product ion; CE, collision energy.

Ethics Committee (IAEC) at the CSIR-Central Drug Research Institute, Lucknow, with approval number IAEC/2020/94/Renew-1/Dated-29.06.2021.

Conflicts of interest

There are no conflicts to declare.

Acknowledgements

The authors are thankful to the Director, CSIR-CDRI, for providing the necessary research facilities. A. R. P. is thankful to the Department of Science and Technology for the Inspire fellowship (No. 2017/IF170800) and A. C. B. sincerely acknowledge ICMR, New Delhi for fellowship. The authors acknowledge the contribution of Ms. Shikha Mishra in antifilarial assays. The authors are also thankful to the in-house Sophisticated Analytical Instrumentation Facility & Research (SAIF & R) for providing the required spectral data. This manuscript has CDRI Communication no. 10574.

References

1 M. A. Bazin, S. Cojean, F. Pagniez, G. Bernadat, C. Cavé, I. Ourliac-Garnier, M. R. Nourrisson, C. Morgado, C. Picot, O. Leclercq, B. Baratte, T. Robert, G. F. Späth, N. Rachidi, S. Bach, P. M. Loiseau, P. Le Pape and P. Marchand, *Eur. J. Med. Chem.*, 2021, **210**, 112956.
2 P. Desjeux, *Comp. Immunol., Microbiol. Infect. Dis.*, 2004, **5**, 305–318.
3 A. Upadhyay, P. Kushwaha, S. Gupta, R. P. Dodda, K. Ramalingam, R. Kant, N. Goyal and K. V. Sashidhara, *Eur. J. Med. Chem.*, 2018, **154**, 172–181.
4 S. Antinori, L. Schifanella and M. Corbellino, *Eur. J. Clin. Microbiol. Infect. Dis.*, 2012, **2**, 109–118.
5 J. I. Manzano, J. Konstantinović, D. Scaccabarozzi, A. Perea, A. Pavić, L. Cavicchini, N. Basilico, F. Gamarro and B. A. Šolaja, *Eur. J. Med. Chem.*, 2019, **180**, 28–40.
6 A. Upadhyay, P. Chandrakar, S. Gupta, N. Parmar, S. K. Singh, M. Rashid, P. Kushwaha, M. Wahajuddin, K. V. Sashidhara and S. Kar, *J. Med. Chem.*, 2019, **11**, 5655–5671.
7 D. Dheer, V. Singh and R. Shankar, *Bioorg. Chem.*, 2017, **71**, 30–54.
8 E. S. Elkhayat, S. R. Ibrahim, G. A. Mohamed and S. A. Ross, *Nat. Prod. Res.*, 2016, **7**, 814–820.
9 P. Misra, K. V. Sashidhara, S. P. Singh, A. Kumar, R. Gupta, S. S. Chaudhaery, S. S. Gupta, H. K. Majumder, A. K. Saxena and A. Dube, *Br. J. Pharmacol.*, 2010, **5**, 1143–1150.
10 P. Pillay, R. Vleggaar, V. J. Maharaj, P. J. Smith, C. A. Lategan, F. Chouteau and K. Chibale, *Phytochemistry*, 2007, **68**, 1200–1205.
11 A. Byczek-Wyrostek, R. Kitel, K. Rumak, M. Skonieczna, A. Kasprzycka and K. Walczak, *Eur. J. Med. Chem.*, 2018, **150**, 687–697.
12 Y. Yamano, Y. Fujita, Y. Mizuguchi, K. Nakagawa, T. Okano, M. Ito and A. Wada, *Chem. Pharm. Bull.*, 2007, **55**, 1365–1370.
13 E. Lattmann, N. Sattayasai, C. S. Schwalbe, S. Niamsanit, D. C. Billington, P. Lattmann, C. A. Langley, H. Singh and S. Dunn, *Curr. Drug Discovery Technol.*, 2006, **3**, 125–134.
14 Ashutosh, S. Gupta, Ramesh, S. Sundar and N. Goyal, *Antimicrob. Agents Chemother.*, 2005, **9**, 3776–3783.
15 G. D. Muylder, K. K. H. Ang, S. Chen, M. R. Arkin, J. C. Engel and J. H. McKerrow, *PLoS Neglected Trop. Dis.*, 2011, **5**, e1253.
16 C. Hansen and E. W. Hansen, *Biol. Trace Elem. Res.*, 2011, **144**, 234–243.
17 P. Shaked-Mishan, N. Ulrich, M. Ephros and D. Zilberstein, *J. Biol. Chem.*, 2001, **276**, 3971–3976.
18 H. Kolodziej and A. F. Kiderlen, *Phytochemistry*, 2005, **66**, 2056–2071.
19 T. Mosmann, *J. Immunol. Methods*, 1983, **65**, 55–63.
20 S. Singh, R. K. Srivastava, M. Srivastava, S. K. Puri and K. Srivastava, *Exp. Parasitol.*, 2011, **127**, 318–321.
21 S. Misra-Bhattacharya, D. Katiyar, P. Bajpai, R. P. Tripathi and J. K. Saxena, *Parasitol. Res.*, 2004, **92**, 177–182.
22 Molinspiration Cheminformatics free web services, **https://www.molinspiration.com**, Slovensky Grob, Slovakia.
23 *XXIV, U. P. The United State of Pharmacopoeia Convention*, Rockville, Maryland, 2000, p. 185.
24 A. R. Pandey, S. Ahmad, S. P. Singh, A. Mishra, A. C. Bisen, G. Sharma, I. Ahmad, S. K. Shukla, R. S. Bhatta, S. Kanojiya, A. Kumar Tamrakar and K. V. Sashidhara, *Phytochemistry*, 2022, **201**, 113286.

